Korean Journal of Remote Sensing, Vol.19, No.1, 2003, pp.11~19

Tropospheric Ozone Retrieval Algorithm Based on the TOMS Scanning Geometry

Jae-Hwan Kim*, Sun-Mi Na*, and M. J. Newchurch**

Department of Atmospheric Sciences, Pusan National University*, Korea
Department of Atmospheric Science, University of Alabama in Huntsville**, USA

Abstract : This paper applies the Scan-Angle Method (SAM) to the Total Ozone Mapping Spectrometer (TOMS) aboard Earth Probe (EP) satellite for determining tropospheric ozone based on TOMS scan geometry. In the northern tropical Africa burning season, the distribution of the SAM-derived tropospheric ozone presents a tropospheric ozone enhancement related to biomass burning. This distribution is consistent with that of fire counts observed from Along Track Scanning Radiometer (ATSR) and that of carbon monoxide, the tropospheric ozone precursor, observed from Measurements of Pollution In The Troposphere (MOPITT). However, this feature is not shown in the distribution of tropospheric ozone derived from other TOMS-based algorithms for the northern burning season. In the high latitudes, the influence of pollution in the SAM results is seen over the northern continents in agreement with carbon monoxide for northern summer when the dynamical activity is weak in the northern hemisphere.

Key Words : Satellite-Based Ozone Retrieval Algorithm, Tropospheric Ozone, TOMS, Biomass Burning.

1. Introduction

Fishman and Larsen (1987) first developed a satellite technique for indirectly measuring the tropospheric column ozone climatology by subtracting the average stratospheric column ozone measured by the Stratospheric Aerosol and Gas Experiment (SAGE) from the total column ozone climatology obtained from the Total Ozone Mapping Spectrometer (TOMS). This technique is called the Tropospheric Ozone Residual (TOR) method. Later, the Convective Cloud Differential (CCD) method produced the direct retrieval by using the difference between the TOMS ozone for high reflectivity ($R > 0.9$) and the TOMS ozone for low reflectivity ($R < 0.2$) (Ziemke *et al.*, 1998). This method assumed that stratospheric ozone is invariant with longitude and concluded that the zonal variation of total ozone determines the zonal variation of tropospheric ozone in the tropics. However, Kim *et al.* (1996) and Newchurch *et al.* (2001) suggested that the zonal wave-one pattern in the TOMS total ozone is due not only to tropospheric ozone but also to stratospheric ozone. The zonal structure of stratospheric ozone is still open question. Kim *et al.* (2001) developed another direct

Received 5 January 2003; Accepted 10 February 2003.

retrieval algorithm, the Scan-Angle Method (SAM), for determining tropical tropospheric ozone from TOMS without any assumption of the zonal structure of stratospheric ozone.

This study uses the SAM algorithm to determine tropospheric ozone. In the tropics, we compare the SAM results with the CCD-derived tropospheric ozone. Because ground ozone monitoring stations are sparse and the frequency of monitoring is very limited, there is no benchmark to evaluate which algorithm is better. Based on the fact that the elevated tropospheric ozone in the tropics is highly correlated with biomass burning activities (Kirchhoff *et al.*, 1996; Olson *et al.*, 1996), we appeal to satellite measurements of fire counts from the Along Track Scanning Radiometer (ATSR) and carbon monoxide, the tropospheric ozone precursor, from Measurements Of Pollution In The Troposphere (MOPITT) aboard Terra satellite. Moreover, we apply the SAM to the high latitudes and compare the SAM-derived tropospheric ozone with the MOPITT-derived CO in the high latitudes.

2. Data

The TOMS experiment aboard the sun-synchronous satellite measures UV radiances backscattered from the atmosphere, earth's surface, and clouds (McPeters *et al.*, 1998). In November 1978, the TOMS flown on Nimbus 7 satellite provided the daily global coverage of the earth's total ozone. At present, the TOMS aboard the Earth Probe (EP) satellite provides us total ozone data. The EP/TOMS satellite operated at a relatively low orbit of 500km and provided the higher spatial resolution from July 1996 through December 1997 and then was boosted to the higher orbit of 750km to obtain complete global coverage (Fig. 1).

The TOMS instrument uses a single monochromatic scanning mirror to sample the backscattered solar ultraviolet radiation at 35 scan positions at 3-degree intervals along a line perpendicular to the orbital plane. It then quickly returns to the first position, not making measurements on the retrace. Fig. 1 illustrates the resulting instantaneous fields of view (IFOV) on the

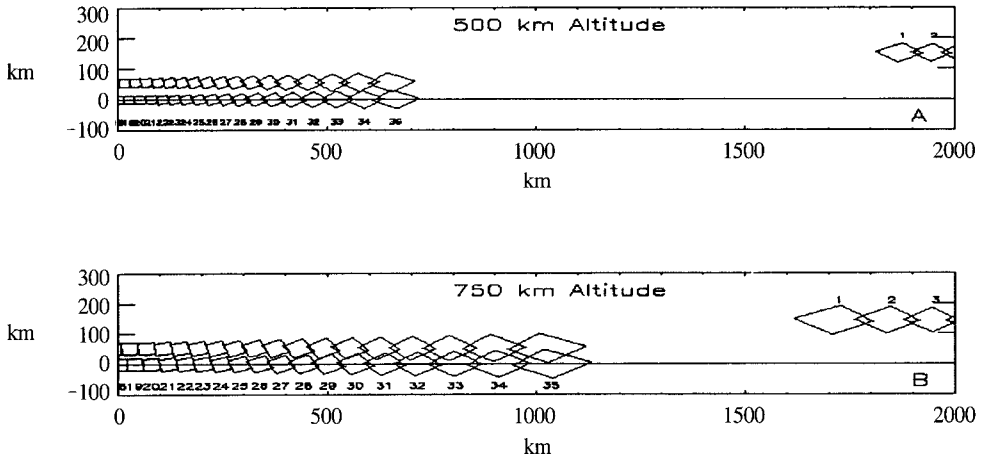

Fig. 1. Earth Probe TOMS instantaneous field of view projected onto Earth's surface; A) 500km orbit altitude, and B) 750km orbit altitude (McPeters *et al.*, 1998).

Earth's surface for adjacent scans and adjacent orbits. Scan positions 1, 18, and 35 correspond to highest scan position to the right, nadir, and highest scan position to the left, respectively. In the SAM, scan positions of 1, 2, 3, 33, 34, and 35 are defined as the high scan position, and scan positions of 16, 17, 18, 19, and 20 as the nadir scan position.

3. Methods

The SAM is the algorithm for retrieving tropospheric ozone based on the variation of retrieval efficiency for tropospheric ozone as a function of scan angle in the TOMS algorithm (Kim *et al.*, 2001). The retrieved total ozone at the nadir position is always closer to truth relative to the ozone at the high scan position. If the actual tropospheric ozone is less than the TOMS *a priori* - tropospheric assumption, then the total ozone retrieved at the high scan positions will be greater than the ozone retrieved at the nadir position. On the other hand, if the actual tropospheric ozone is greater than the TOMS assumption, then the retrieval at the high scan positions will be less than at the nadir retrieval. The normalized differences between total ozone averaged over high-scan positions and over nadir-scan positions (hereafter *diff*) as a function of altitude are calculated (Fig. 2). The averaging kernel shows that most of signals come from the troposphere with a peak at 5-km altitude.

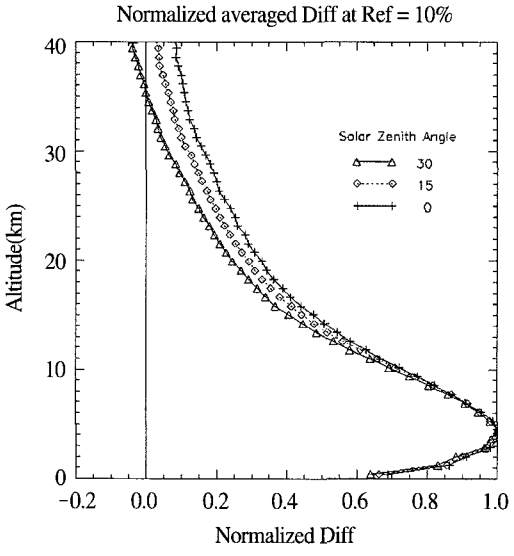

Fig. 2. Difference in tropospheric ozone retrieval efficiency between nadir observation positions and high scan positions normalized to the peak difference. Reflectivity and azimuth angle are 10% and 135 degrees, respectively (Kim *et al.*, 2001).

Because the TOMS instrument does not measure simultaneously at both nadir and high scan positions, we calculate the monthly averaged *diff* over the 2° latitude and 10° longitude box. The *diff* over the selected box is the sum of the error due to the tropospheric ozone retrieval efficiency and the daily variation of stratospheric ozone between two scanning positions. If the daily stratospheric ozone variation is smooth, the contribution from stratospheric ozone will be canceled out on the monthly mean *diff* and thereby the tropospheric ozone signal will be obtained. However, if there is a rapid and enormous change in the daily stratospheric ozone variation, the tropospheric ozone signal in the *diff* will be seriously contaminated. If the effect of stratospheric ozone is canceled out, the *diff* is in the range between ± 5. We utilize these values of the *diff* as the criteria for application of the SAM algorithm. In the tropics, no values less than -5 and greater than $\pm$ 5 occur because of the weak dynamical activity in the stratosphere without season (Fig. 3a and Fig. 3b). Because the dynamical activity in the high latitudes depends on season and latitude, we need to investigate the seasonal and latitudinal dependence of the *diff*. For northern winter, the *diff* amplitude in Fig. 3a is larger in the northern hemisphere than in the southern hemisphere because the dynamical activity is strong in the northern hemisphere (Holton, 1992). On the contrary, for southern winter, the *diff* amplitude in Fig. 3b is larger in the latter than in the former because dynamical activity

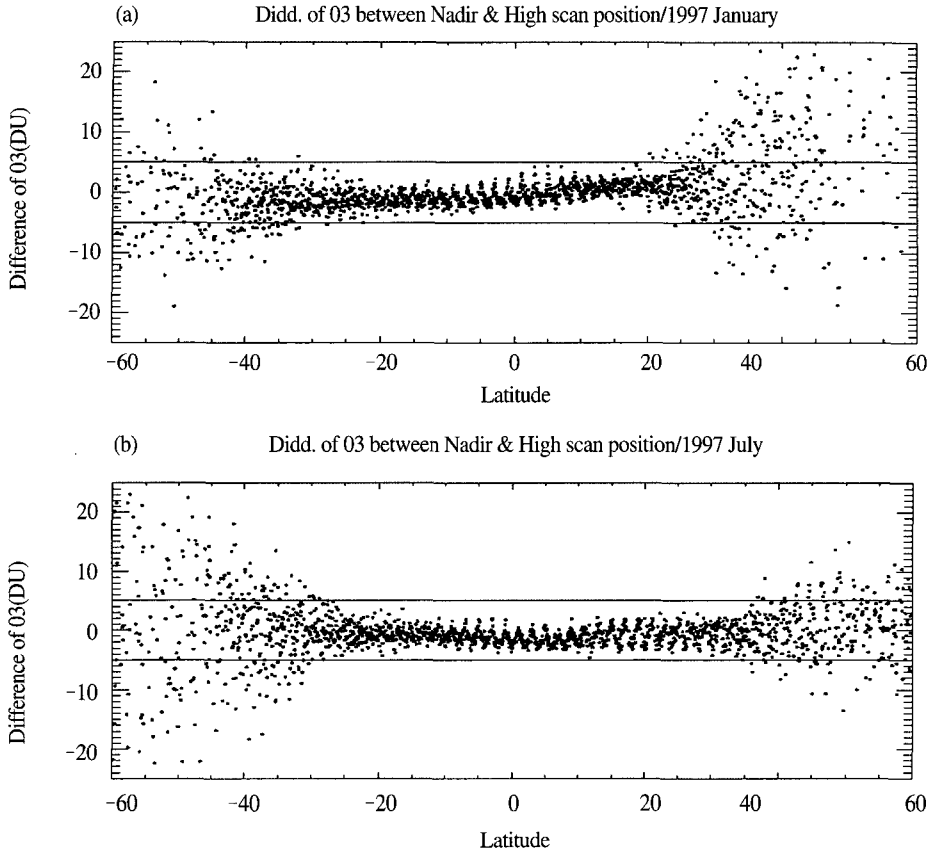

Fig. 3. Latitudinal variation of total ozone difference between nadir and high scan positions in (a) January, and (b) July 1997.

is strong in the southern hemisphere. Even though the applicable extent of the SAM algorithm in the high latitudes depends on season and latitude, the *diff* amplitude is well correlated with the dynamic activity in the stratosphere as a function of season. The tropical region is the best place for application of the SAM algorithm over the year round.

Therefore, *diff* can be used to detect the signal from tropospheric ozone for the weak dynamical activity in the stratosphere. The derived relationship between *diff* and the actual tropospheric ozone amount is as follows:

$$\text{Tropospheric ozone column} = 32 + 6.7 \times diff$$

Where 32 DU is TOMS tropical tropospheric ozone *a priori* climatology and 6.7 is the scale factor. The magnitude of that scale factor varies from approximately 5 to 8 and averages 6.7 for the case that TOMS tropospheric ozone *a priori* climatology is 32 DU (Kim *et al.*, 2001).

4. Tropospheric Ozone in the Tropics

Fig. 4a shows the distribution of tropospheric ozone derived from the SAM by using EP/TOMS data from December 1996 to February 1997, which corresponds to the northern burning season. White areas over the southern America in this figure are cloudy regions. The maximum amounts of tropospheric ozone are observed over the northern equatorial Africa. Because the

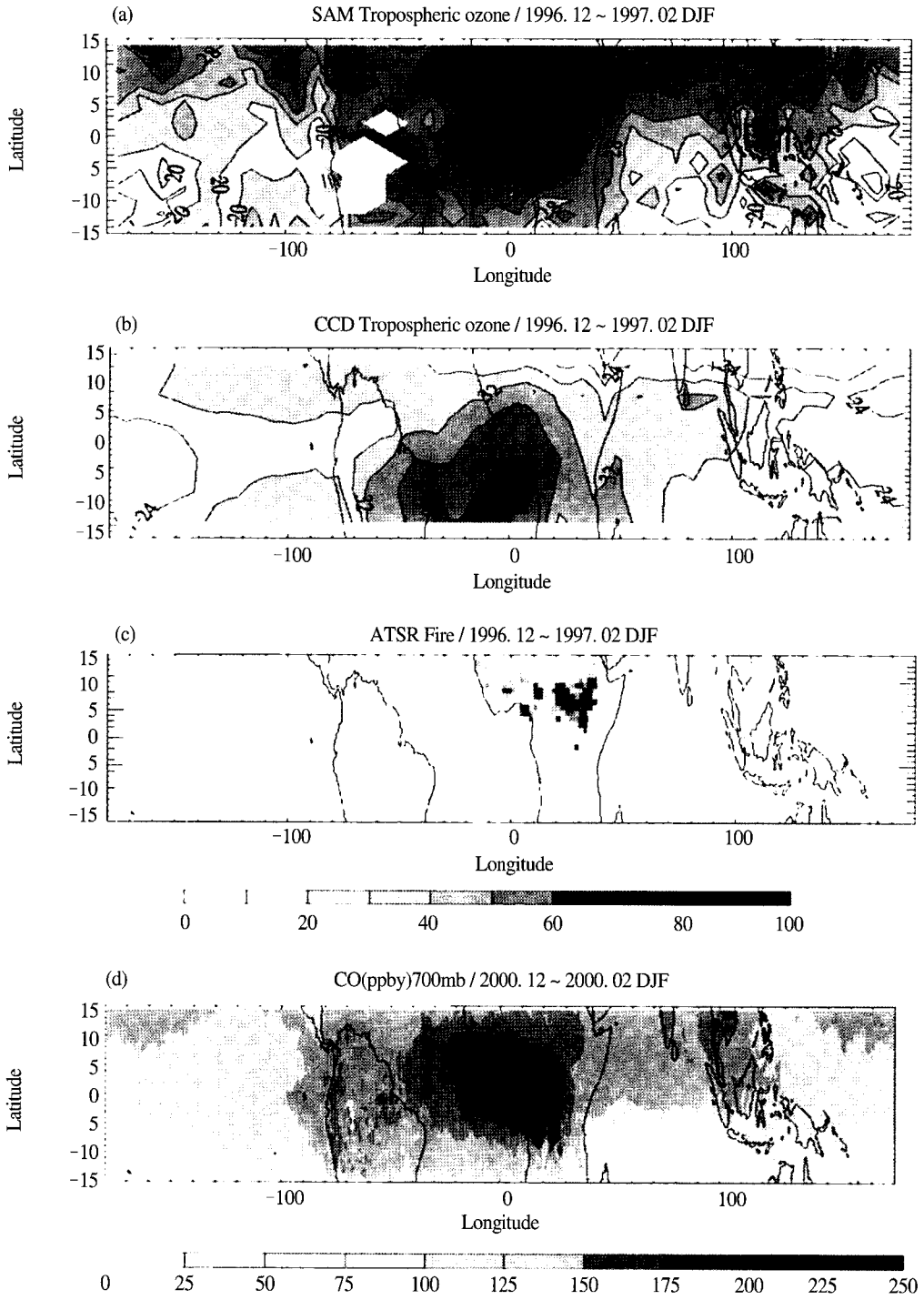

Fig. 4. Distribution of (a) tropospheric column ozone (Dobson Unit, DU) derived from the SAM, (b) tropospheric ozone derived from the CCD method, (c) fire counts from ATSR for December 1996 to February 1997, and (d) CO from MOPITT for December 2000 to February 2001.

elevated ozone is generally observed over continent and island, and the lowest ozone is observed over the remote oceanic area, the elevated ozone appears to be related to anthropogenic emissions of ozone precursors.

Fig. 4b shows the CCD-derived tropospheric ozone for the same period as for Fig. 4a. The maximum ozone is observed over the southern tropical Atlantic. This distribution is very different from the SAM results. It is very striking to see that the amounts of tropospheric ozone from the northern tropical Africa across India to Indochina with relatively high anthropogenic emission are as low as over remote oceanic areas with no source of ozone precursors.

Fig. 4c shows the total fire counts from ATSR for the same period as for Fig. 4a and Fig. 4b. It shows the broad intensive burning activity over the northern Africa and weak burning over the limited area in the southern America and Indochina. No noticeable burning activity is observed over the southern tropical Africa. The extensive field campaigns over the southern America and Africa, Atmospheric Boundary Layer Experiment (ABLE) and Transport and Atmospheric Chemistry in the Atlantic (TRACE-A), show that the elevated ozone over the southern America and Africa is strongly correlated with biomass burning (Talbot *et al.*, 1986; Andreae *et al.*, 1988; Andrea *et al.*, 1996). Therefore, the maximum tropospheric ozone over the northern equatorial Africa for December-February observed from the SAM results agrees well with the intensive burning activity. On the contrary, the tropospheric ozone distribution from CCD is poorly correlated with the distribution of burning activity.

In order to find the ozone sources other than biomass burning, we use carbon monoxide measured from MOPITT as the proxy for the precursors of photochemically produced ozone. Fig. 4d shows the MOPITT-derived CO measurement in the low troposphere for December 2000 to February 2001 that is different from the period used in Fig. 4a-c, because MOPITT began to measure CO on March 2000. The maximum CO is observed over the northern equatorial Africa, which is highly correlated with the burning activity seen in Fig. 4c. This maximum location is well correlated with the SAM results, but poorly correlated with the CCD results.

5. Tropospheric Ozone in the High Latitudes

Fig. 5a shows the distribution of tropospheric ozone derived from the SAM between 20S and 35N for July 1997. Because the dynamical activity in the stratosphere for northern summer is weak in the northern hemisphere than in the southern hemisphere as discussed in the section 3, the SAM algorithm can capture the signal of tropospheric ozone over higher latitudinal regions in the northern hemisphere than in the southern hemisphere. In order to analyze the SAM-derived tropospheric ozone in the high latitudes, we utilize carbon monoxide from the MOPITT as the precursor of tropospheric ozone. Because there are no MOPTT CO measurements for the same period as for Fig. 5a, we use MOPITT-derived carbon monoxide for July 2000 (Fig. 5b). The latitudinal distribution of CO shows that the northern area has more CO than the southern area. This latitudinal distribution is correlated with that of tropospheric ozone derived from the SAM. The lower ozone appears over the tropical Pacific, which is the remote oceanic region with no source of tropospheric ozone precursor, in a good agreement with the distribution of CO. The higher ozone from the southern Unites States, across Africa, to southwestern Asia agrees with the MOPITT CO. These northern continents for northern summer appear to be under the influence of polluted air, which is consistent with the study of Fishman *et al.* (1990). In the southern hemisphere, the enhanced tropospheric ozone observed over Australia is in agreement with the enhanced CO,

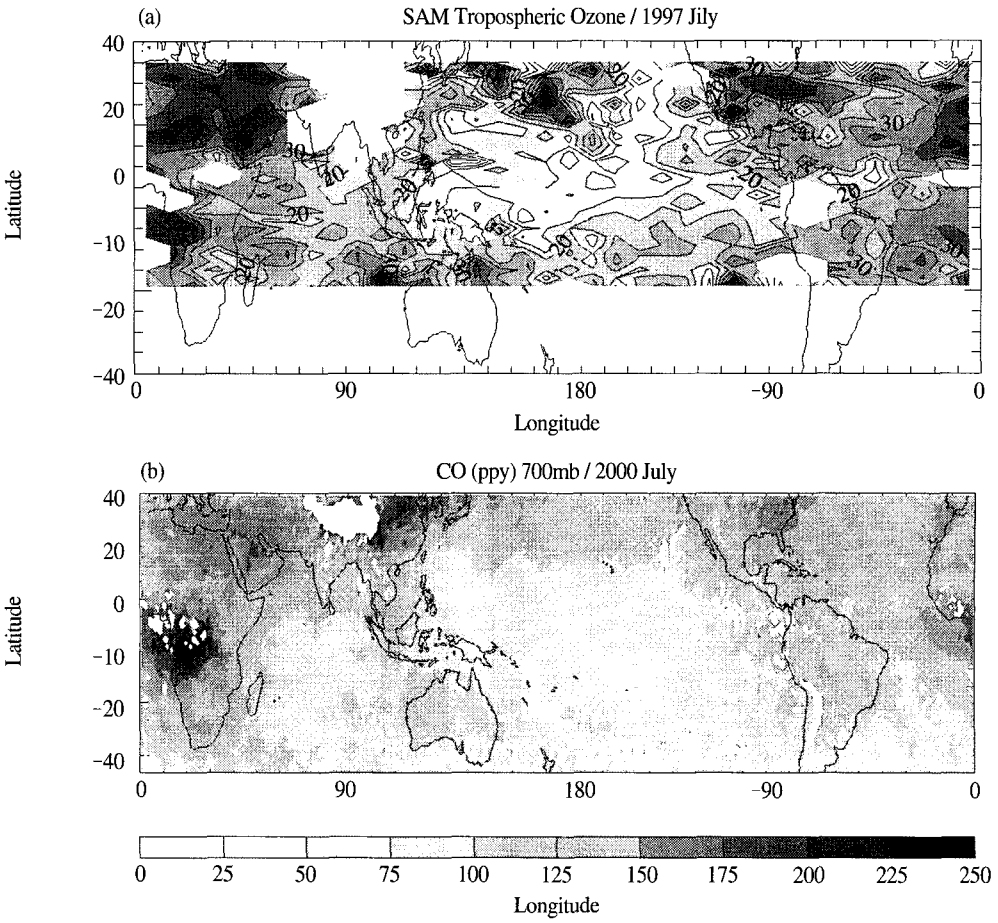

Fig. 5. Distribution of (a) tropospheric column ozone (Dobson Unit, DU) derived from the SAM for July 1997, and (b) CO from MOPITT for July 2000.

which is caused by burning activity (http://shark1.esrin.esa.it/ionia/FIRE/AF/ATSR/).

6. Conclusions

Many researchers have developed algorithms for determining tropospheric ozone from satellite-based instrument with the assumption of zonally flat distribution in stratospheric ozone (Fishman and Larsen, 1987; Fishman *et al.*, 1996; Hudson and Thompson, 1998; Ziemke *et al.*, 1998).

The distribution of tropospheric ozone derived from these algorithms has shown a persistent maximum due to biomass burning over the southern tropical Atlantic for all months of the year. It is well known that the enhancement of tropical tropospheric ozone is strongly correlated with biomass burning activity (Crutzen *et al.*, 1990). Biomass burning activity shifts from the southern tropical America and Africa for July-October period corresponding to the southern burning season to the northern equatorial Africa for December-March period corresponding to the northern burning season. This movement has an effect on the distribution of

tropospheric ozone. Therefore, the elevated tropospheric ozone must be related to biomass burning activity. We expect to observe that the enhancement in the distribution of tropospheric ozone is seen over the southern tropical Atlantic for the southern burning season and over the northern equatorial Africa for the northern burning season. This ozone feature appears to be contradicted to the distribution of tropospheric ozone for the northern burning season derived from these algorithms. Thompson *et al.* (2000) defined this discrepancy as the "tropical Atlantic paradox".

Recently, Kim *et al.* (2001) developed the Scan-Angle Method (SAM) for determining tropospheric ozone using the *diff* based on the TOMS scan-angle geometry. Because the *diff* is affected by the variation of the stratospheric ozone, the way to examine the applicability of the SAM is to check the dynamical activity in the stratosphere. The tropical region is the best place for application of the SAM algorithm over the year round because of the weak dynamical activity. In the high latitudes, however, we restrict this method to the summer hemisphere because of the weak dynamical activity in the summer hemisphere.

In the tropics, the SAM results present higher ozone over the northern equatorial Africa for the northern burning season, which is consistent with the distribution of fire counts measured from ATSR. For the southern burning season, the elevated ozone over the southern Atlantic also agrees well with the distribution of the ATSR fire counts. In the comparison of the SAM results with CO, the SAM results detect the signal from tropospheric enhancement over the northern equatorial Africa for the northern burning season and over the southern Atlantic for the southern burning season. In the high latitudes, the influence of pollution in the SAM results is seen over the northern continents for northern summer when the dynamical activity is weak in the northern hemisphere. This feature is well correlated with the distribution of the MOPITT CO.

Based on the comparison between the SAM-derived tropospheric ozone and the various satellite measurements such as the ATSR fire counts and the MOPITT CO, the SAM algorithm appears to be more reliable algorithm than the residual-based algorithm. The improvement of this algorithm requires the simultaneous measurements at both nadir and high scan positions such as Multi-angle Imaging Spectro-Radiometer (MISR). If this kind of sensor is in operation in the future, we will be able to obtain the daily tropospheric ozone map even in the high latitudes.

Acknowledgments

We thank L. Emmons for providing the MOPITT CO data. This work was supported by Technology in Marine Meteorological and Climatological Data Utilization of Meteorological and Earth quake R&D Program by Korea Meteorological Administration.

References

Andreae, M. O., J. Fishman, and J. Lindesay, 1996. The Southern Tropical Atlantic Region Experiment(STARE): Transport and Atmospheric Chemistry near the Equator- Atlantic(TRACE-A) and Southern African Fire-Atmosphere Research Initiative(SAFARI): An Introduction, *Journal of Geophysical Research,* 101(19): 23519- 23520.

Andreae, M. O., E. V. Browell, M. Garstang, G. L. Gregory, R. C. Harriss, G. F. Hill, D. J. Jacob, M. C. Pereira, G. W. Sachse, A. W. Setzer, P. L. Silva Dias, R. W. Talbot, A. L. Torres, and S. C. Wofsy, 1988. Biomass-burning emissions and associated haze layers over Amazonia, *Journal of Geophysical Research,* 93(2): 1509-1527.

Crutzen, P. J. and M. O. Andreae, 1990. Biomass burning in the tropics: Impact on atmospheric chemistry and biogeochemical cycles, *Science,* 250(21): 1669-1678.

Fishman, J. and J. C. Larsen, 1987. Distribution of total ozone and stratospheric ozone in the tropics: Implication for the distribution of tropospheric ozone, *Journal of Geophysical Research,* 92(6): 6627-6634.

Fishman, J., C. E. Watson, J. C. Larsen, and J. A. Logan, 1990. Distribution of tropospheric ozone determined from satellite data, *Journal of Geophysical Research,* 95(3): 3599-3617.

Fishman, J., V. G. Brackett, E. V. Browell, and W. B. Grant, 1996. Tropospheric ozone derived from TOMS/SBUV measurements during TRACE A, *Journal of Geophysical Research,* 101(19): 24069-24082.

Holton, J. R., 1992. *An introduction to dynamic meteorology,* Academic press, inc.

Hudson, R. D. and A. M. Thompson, 1998. Tropical tropospheric ozone from total ozone mapping spectrometer by a modified residual method, *Journal of Geophysical Research,* 103(17): 22129-22145.

Kim, J. H. and M. J. Newchurch, 1996. Climatology and trends of tropospheric ozone over the eastern Pacific Ocean: The influences of biomass burning and tropospheric dynamics, *Geophysical Research Letters,* 23(25): 3723-3726.

Kim, J. H., M. J. Newchurch, and K. Han, 2001. Distribution of tropical tropospheric ozone determined directly from TOMS measurements, *Journal of the Atmospheric Sciences,* 58(18): 2699-2708.

Kirchhoff, V. W. J. H., J. R. Alves, F. R. da Silva, and J. Fishman, 1996. Observations of ozone concentrations in the Brazilian cerrado during the TRACE-A field expedition, *Journal of Geophysical Research,* 101(19): 24029-24042.

McPeters, R. D. and Coauthors, 1998. *Earth Probe Total Ozone Mapping Spectrometer (TOMS) Data Products User's Guide*, NASA, 1998-206895.

Newchurch, M. J., D. Sun, and J. H. Kim, 2001. Zonal wave-1 structure in TOMS tropical stratospheric ozone, *Geophysical Research Letters.* 28(16): 3151-3154.

Olson, J. R., J. Fishman, V. W. J. H. Kirchhoff, D. Nganga, and B. Cros, 1996. An analysis of the distribution of O3 over the southern Atlantic region, *Journal of Geophysical Research,* 101(19): 24083-24094.

Talbot, R. W., R. C. Harriss, E. V. Browell, G. L. Gregory, D. I. Sebacher, and S. M. Beck, 1986. Distribution and geochemistry of aerosols in the tropical northern Atlantic troposphere: Relationship to Saharan dust, *Journal of Geophysical Research,* 91(4): 5173-5182.

Thompson, A. M., B. G Doddridge, J. C. Witte, R. D. Hudson, W. T. Luke, J. E. Johnson, B. J. Johnson, S. J. Oltmans, and R. Weller, 2000. A tropical Atlantic paradox: Shipboard and satellite views of a tropospheric ozone maximum and wave-one in January-February 1999, *Geophysical Research Letters,* 27(20): 3317-3320.

Ziemke, J. R., S. Chandra, and P. K. Bhartia, 1998. Two new methods for deriving tropospheric column ozone from TOMS measurements: The assimilated UARS MLS/HALOE and convective-cloud differential techniques, *Journal of Geophysical Research,* 103(17): 22115-22128.